Thermochemical and Cyclability Analyses of the CO_2 Absorption Process on a Ca/Al Layered Double Hydroxide

Heriberto Pfeiffer[1]; Tatiana Ávalos-Rendón[2]; Enrique Lima[3]; and Jaime S. Valente[4]

Abstract: Hydrocalumite ($[Ca_2Al(OH)_6]_2CO_3 \cdot mH_2O$) was synthesized by precipitation and thermally activated at 300 and 550°C. Its CO_2 chemisorption capacity was evaluated and compared with that of calcium oxide (CaO). Initial thermal analyses showed that CaAl-550 sample has better properties as CO_2 sorbent than CaO, evaluated under similar conditions. It was determined that both materials (CaAl-550 and CaO) have similar kinetic behavior, and the presence of $Ca_{12}Al_{14}O_{33}$ on the CaAl-550 sample did not reduce or interfere with the CO_2 capture. Moreover, when the CO_2 absorption-desorption cyclability was analyzed, the CaAl-550 sample apparently possessed better CO_2 capture efficiency and thermal stability than CaO. In fact, different characterization analyses (nuclear magnetic resonance and scanning electron microscopy) suggest that CO_2 capture efficiency and thermal stability observed on the CaAl-550 sample can be attributed to the aluminum presence, as $Ca_{12}Al_{14}O_{33}$. **DOI: 10.1061/(ASCE)EE.1943-7870.0000429.** © *2011 American Society of Civil Engineers.*

CE Database subject headings: Absorption; Carbon dioxide; Kinetics; Temperature effects; Thermal analysis.

Author keywords: Absorption; Carbon dioxide; Kinetics; Temperature effects; Thermal analysis.

Introduction

The removal and recovery of CO_2 from hot gas streams is one of the most important environmental issues to be solved in the near future (Friedmann 2007; Pawlesa et al. 2007). Therefore, different kinds of materials, such as zeolites, organic materials, minerals, polymers, layered double hydroxides, oxides, and ceramics, among others, have been tested as CO_2 sorbents, using physical or chemical mechanisms (Maceiras et al. 2008; Mosqueda et al. 2006; Romeo et al. 2008; Chen et al. 2008; Díaz et al. 2008; Nomura et al. 2000; Park et al. 2002; Seo et al. 2009; Macario et al. 2005; Yavuz et al. 2009; Lwin and Abdullah 2009; Nair et al. 2009). Among these materials, different ceramics containing alkaline or alkaline earth elements have shown great potential (Ávalos-Rendon et al. 2009; Alcérreca-Corte et al. 2008; Ochoa Fernández et al. 2009; Nair et al. 2004; Preda et al. 2009; Liu et al. 2010; Chen et al. 2009; Yang et al. 2009). In general, these ceramics trap CO_2 through a chemical reaction, absorption, in which the respective carbonate is produced. Usually, they are able to absorb CO_2 in a relatively wide temperature range (from approximately 300–400°C up to 800°C). Among them, calcium oxide (CaO) has been reported to possess very good properties (Chen et al. 2009; Yang et al. 2009; Manovic and Anthony 2009; Li et al. 2009; Martavaltzi and Lemonidou 2008; Lu et al. 2009).

Layered double hydroxides (LDHs) are also suitable as CO_2 sorbents, through two different mechanisms: adsorption at low temperatures, or absorption at high temperatures. LDHs are mixed metal hydroxides represented by the general formula $[M^{II}_{1-x}M^{III}_x(OH)_2]^{x+}(A^{n-})_{x/n} \cdot mH_2O$, where M^{II} and M^{III} stand for divalent and trivalent cations occupying octahedral sites within the hydroxyl layers, x is equal to the ratio $M^{III}/(M^{II}+M^{III})$ and takes values in the range of 0.20 to 0.50, and A^{n-} is an exchangeable interlayer anion. These materials have received considerable attention in recent years because they have a wide range of applications, primarily as catalysts and catalyst precursors (Lima et al. 2004; Segni et al. 2006; Kirkpatrick et al. 1999), where the Mg-Al-CO_3 LDH, known as hydrotalcitelike, has been the most widely studied. Within the LDH family, however, there are other compositions. For instance, the $[Ca_2Al(OH)_6]_2CO_3 \cdot mH_2O$, a hydrocalumite-like compound, is a LDH with a well ordered CaAl distribution in the hydroxide layers, while the anions and water are highly ordered in the interlayer spaces. In hydrocalumite, trivalent aluminum cations remain, as in hydrotalcites, six-fold coordinated. Calcium cations are coordinated to six OH groups, and interlayer water is also directly coordinated to calcium, thus creating sevenfold-coordinated Ca. Then, interlayer water occupies certain ordered positions, which yields a well defined anionic structural environment. Ordering of cations, anions, and water is the primary difference between hydrocalumite and hydrotalcite. Another interesting difference is that thermal decomposition of hydrotalcite yields high surface area mixed oxides that expose strong Lewis base sites. On the other hand, hydrocalumite is transformed into a mixture of CaO and mayenite $Ca_{12}Al_{14}O_{33}$ (Martavaltzi and Lemonidou 2008; Manovic and Anthony 2010). Thus, ordering of cations in hydrocalumite and its thermal decomposition could

[1]Senior Lecturer, Instituto de Investigaciones en Materiales, Universidad Nacional Autónoma de México, Circuito exterior s/n, Cd. Universitaria, Del. Coyoacán, CP 04510, México DF, Mexico (corresponding author). E-mail: pfeiffer@iim.unam.mx

[2]Ph.D. candidate, Instituto de Investigaciones en Materiales, Universidad Nacional Autónoma de México, Circuito exterior s/n, Cd. Universitaria, Del. Coyoacán, CP 04510, México DF, Mexico.

[3]Senior Lecturer, Instituto de Investigaciones en Materiales, Universidad Nacional Autónoma de México, Circuito exterior s/n, Cd. Universitaria, Del. Coyoacán, CP 04510, México DF, Mexico.

[4]Senior Lecturer, Instituto Mexicano del Petróleo, Eje Central 152, CP 07730, México D.F., Mexico.

Note. This manuscript was submitted on June 1, 2010; approved on May 17, 2011; published online on May 18, 2011. Discussion period open until April 1, 2012; separate discussions must be submitted for individual papers. This paper is part of the ***Journal of Environmental Engineering***, Vol. 137, No. 11, November 1, 2011. ©ASCE, ISSN 0733-9372/2011/11-1058–1065/$25.00.

J. Environ. Eng. 2011.137:1058-1065.

probably endow it with different properties regarding basicity, stability, and basic site density that may endow these materials with interesting adsorption properties.

The CO_2 absorption capacities on different CaAl systems have been reported previously (Martavaltzi and Lemonidou 2008; Manovic and Anthony 2009, 2010; Lu et al. 2006). The primary goals of these previous works have been: (1) to investigate the synthesis of different materials, such as CaO-Al_2O_3 or CaO-$Ca_{12}Al_{14}O_{33}$ powders, or even the preparation of calcium aluminate pellets; and (2) to evaluate their CO_2 absorption feasibility and efficiency in terms of the number of absorption-desorption cycles. In general, all these materials presented encouraging properties. Some of the conclusions drawn from these investigations are: (1) the presence of aluminum oxides as $Ca_{12}Al_{14}O_{33}$ has a strong beneficial effect on sorbent performance during CO_2 capture cycles (Manovic and Anthony 2010); (2) it seems that aluminate cements are a good source of aluminum oxide for the preparation of nanoporous structures, which enhances the CO_2 absorption (Manovic and Anthony 2009); (3) calcium aluminate pellets present superior carbonation at longer times (Manovic and Anthony 2010).

Therefore, the aim of this work was to evaluate CO_2 sorption using the Ca-Al-CO_3 LDH (hydrocalumite) as starting material. Its calcination product presents a chemical composition similar to the materials mentioned previously, but with a different structural conformation. The samples were characterized by several techniques, such as X-ray diffraction (XRD), N_2 physisorption, ^{27}Al magic angle spinning (MAS) nuclear magnetic resonance spectroscopy (NMR), and scanning electron microscopy (SEM). Different dynamic and isothermal analyses were performed to investigate the CO_2 absorption process on this material. Additionally, for comparison purposes, some CO_2 absorption experiments were also performed on CaO.

Experimental

The synthesis of hydrocalumite was performed by preparing a 1 M aqueous solution containing the required amounts of $Ca(NO_3)_2 \cdot 4H_2O$ and $Al(NO_3)_3 \cdot 9H_2O$, with a Ca/Al molar ratio of 2. Separately, a 2 M alkaline solution was prepared with KOH and K_2CO_3. Both solutions were added dropwise and simultaneously to a glass reactor, under constant stirring, at a fixed pH of 12. The white precipitate was aged at 80°C for 18 h under constant mechanical stirring. Afterward, the product was thoroughly washed with hot deionized water to eliminate undesirable counterions, and dried at 100°C for 24 h. Two different portions of the hydrocalumite sample were thermally activated at 300 and 550°C for 4 h before CO_2 capture tests; these samples were labeled as CaAl-300 and CaAl-550, respectively. For comparison purposes and to fully understand the CO_2 absorption on hydrocalumite, CaO was also tested as CO_2 sorbent. It was prepared by calcining calcium hydroxide [$Ca(OH)_2$, Sigma-Aldrich] at 750°C for 30 min. Afterward, the CaO composition was corroborated by XRD (data not shown).

Materials obtained before and after the calcination processes were characterized by XRD, using a diffractometer Siemens D-5000 coupled to a copper anode X-ray tube. The presence of different crystalline phases was confirmed by fitting the diffraction pattern with the corresponding Joint Committee Powder Diffraction Standards (JCPDS). Additionally, the surface area of the samples was determined by N_2 adsorption, using the BET model (Rouquerol et al. 1999). The equipment used in this case was a Minisorp II from Bel-Japan, at −196 °C, using a multipoint technique. Samples were previously outgassed in vacuum. The different samples were further characterized by thermogravimetric analysis (TGA), performed in a Q500HR thermobalance from TA Instruments. In particular, the native and the two activated samples were dynamically analyzed from room temperature to 800°C at a heating rate of 3 °C/min, with a CO_2 flow of 60 mL/min. Other activated samples were isothermically studied at different temperatures using the same CO_2 flow. Finally, the recyclability of the materials was tested at different temperatures. To verify the reproducibility of the results, some randomly chosen experiments were repeated, in all cases obtaining variations of no more than ±2%. Some of the experiments repeated are presented in the corresponding figures with their error bars.

Some of the samples were also characterized, before and after the CO_2 absorption process, by solid state NMR and SEM. ^{27}Al MAS NMR spectra were acquired with a 4 mm probe on an Avance II Bruker spectrometer at a frequency of 78.15 MHz. Short single pulses of $\pi/12$, pulse delays of 0.5 s, and a spinning speed of 10 kHz were used for the data collection. Chemical shifts are referenced to aqueous 1 N $AlCl_3$ solution. Scanning electron micrographs were obtained in a Cambridge Leica Stereoscan 440 equipment, where samples were previously coated with gold to avoid lack of conductivity.

Results and Discussion

Fig. 1 presents the XRD patterns of the native and thermally activated hydrocalumite samples. The XRD pattern of the native hydrocalumite sample fitted to the 78-1219 JCPDS file, indicating that hydrocalumite is the only phase present in the sample, at least within XRD detection level. Then, in the activated samples, the hydrocalumite phase was no longer detected, and the obtained XRD patterns were similar to each other, with some differences. The sample activated at 300°C showed the formation of a mixture of amorphous and crystalline phases, where the crystalline phases detected were calcium oxide (CaO, JCPDS file 37-1497), calcium aluminum oxide (so called mayenite, $Ca_{12}Al_{14}O_{33}$, JCPDS file 48-1882), and calcium carbonate as calcite ($CaCO_3$, JCPDS file 05-0586). Calcium oxide and mayenite correspond to the hydrocalumite decomposition, whereas $CaCO_3$ must be produced during the thermal activation process, owing to the reaction of calcium with the carbonate anions initially present in the sample. Finally, the sample activated at 550°C is composed of CaO and $Ca_{12}Al_{14}O_{33}$ as well, whereas the amorphous phase and $CaCO_3$

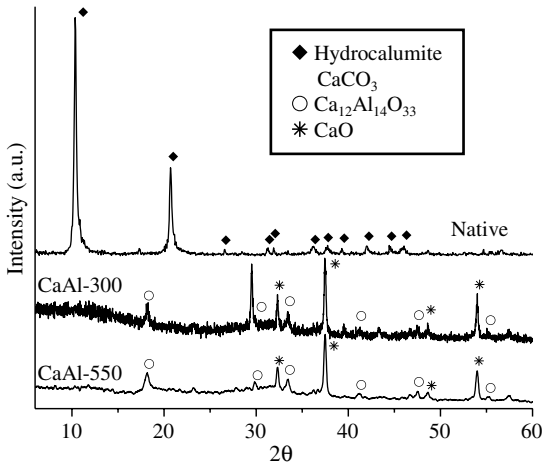

Fig. 1. XRD patterns of hydrocalumite before and after different thermal activation processes

J. Environ. Eng. 2011.137:1058-1065.

have practically disappeared. Therefore, the amorphous phase detected in CaAl-300 must have been a mixture of both metal oxides that crystallized at higher calcination temperature. On the other hand, $CaCO_3$ must have decomposed, producing CO_2 and CaO.

After the structural characterization, the native and activated hydrocalumite samples were thermally analyzed under different atmospheres (Fig. 2). Initially, native hydrocalumite was thermally analyzed under air atmosphere (hydrocalumite-Air). This thermogram initially shows, between room temperature and 100°C, a weight loss of approximately 9 wt%, which corresponds to a dehydration process of the H_2O molecules located between the hydrocalumite structural layers. Then, a second weight loss was observed between 215 and 300°C. Here, the sample lost 13 wt%, owing to the dehydroxilation process of the sample. Finally, the sample presented a third weight loss stage, between 460 and 600°C. In this case, as the sample produced $CaCO_3$, according to the XRD results, the loss is ascribed to the $CaCO_3$ decomposition process.

Afterward, the native and activated samples were thermally evaluated under a CO_2 atmosphere. The native sample (hydrocalumite-CO_2) presented similar dehydration and dehydroxilation processes to those observed on air. However, in this case, the sample did not lose weight because of decarbonation. Instead, it gained weight between 375 and 475°C, which may correspond to the carbonation of the calcium oxides. Finally, the decarbonation process began at approximately 480°C.

The activated samples presented interesting behaviors when they were thermally tested in a CO_2 atmosphere. None presented the dehydration or dehydroxilation processes and both samples absorbed CO_2, as expected. Nevertheless, the CO_2 absorption process was different in each case. Whereas the CaAl-300 sample absorbed CO_2 between 150 and 480°C, the CaAl-550 sample absorbed CO_2 between 200 and 540°C. Additionally, although it is a dynamic process, the CaAl-300 sample absorbs more CO_2 than the CaAl-550 sample.

The thermogram of CO_2 absorption on pure CaO (CaO-CO_2) is also presented, for comparison purposes, in Fig. 2. CaO began to absorb CO_2 at approximately 200°C and the absorption is clearly divided in two different stages as a function of temperature. Between 200 and 380°C, an initial weight increment was observed that changed its slope at higher temperatures. The initial process must correspond to the CO_2 absorption over the surface of the CaO particles. Then, when a $CaCO_3$ external layer is produced, a diffusion process is required to continue the CO_2 capture, now into the bulk of the CaO particles, where the diffusion process is importantly enhanced at higher temperatures. All these results are in good agreement with different reports in which it has been probed that CaO and $CaCO_3$ are able to absorb CO_2 in this temperature range (Choi et al. 2009; Bhatia and Perlmutter 1983).

To further analyze the CO_2 absorption process on the activated hydrocalumite samples, different isothermal experiments were performed on both activated samples (Figs. 3 and 4). Initially, the CaAl-300 sample was isothermically analyzed between 250 and 500°C (Fig. 3). At 250 and 300°C, an exponential behavior was observed, but the amount of CO_2 absorbed was minimal, less than 1 wt% after 3 h. The amount of absorbed CO_2 increased considerably when the CO_2 flow temperature was set at 350 and 400°C. In these cases, samples absorbed 2.4 and 7.7 wt%, respectively, in the same time period. Unexpectedly, when working at 450 and 500°C, a different behavior was observed. Although these samples showed the fastest CO_2 absorption at short times [Fig. 3(b)], absorbing 4 wt% of CO_2, the total CO_2 absorption was less than that measured at lower temperatures (350 and 400°C). This is because above 400°C, the $CaCO_3$ present in this sample decomposes, as supported by the XRD results. Then, a CO_2 desorption process was activated. In fact, at these specific conditions, the CaAl-300 sample is chemisorbing CO_2, but at the same time, the $CaCO_3$ remnant must decompose, desorbing CO_2.

On the other hand, the sample activated at 550°C (CaAl-550) presented a totally different behavior (Fig. 4). In this case, the

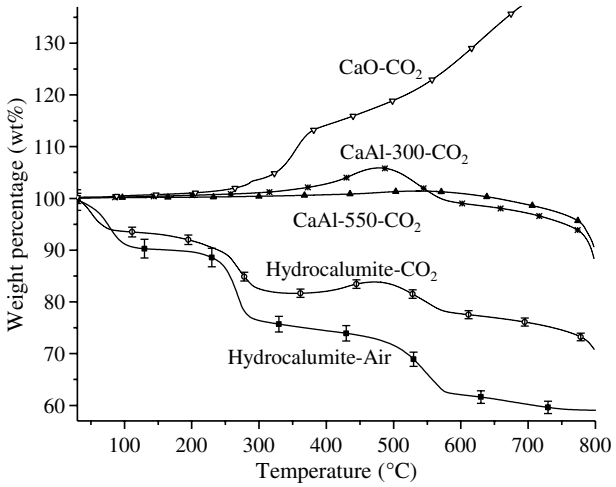

Fig. 2. Thermogravimetric analyses of the hydrocalumite (before and after different thermal activation processes) and CaO, under different atmospheres

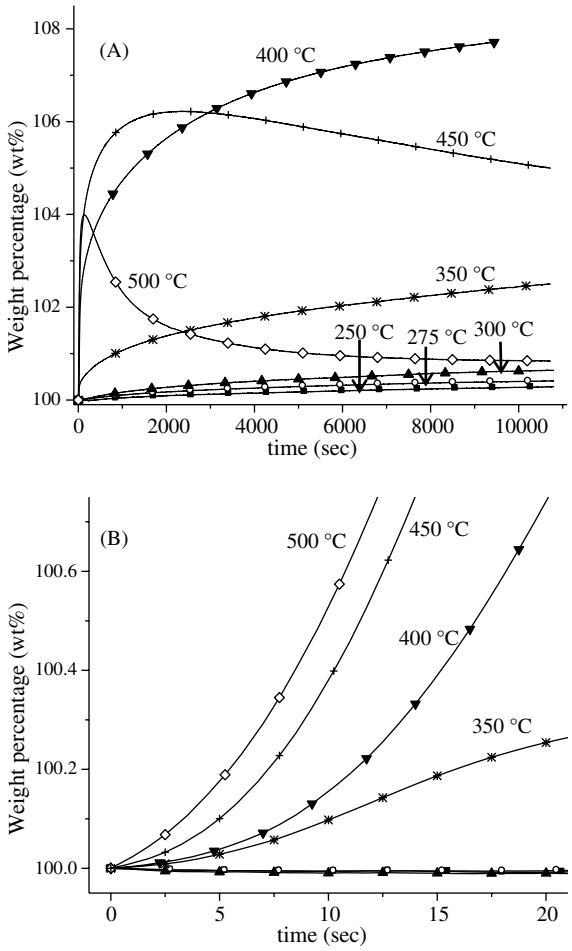

Fig. 3. (a) Isotherms of CO_2 absorption on the CaAl-300 sample at different temperatures; (b) first 20 s of the same isothermal experiments

J. Environ. Eng. 2011.137:1058-1065.

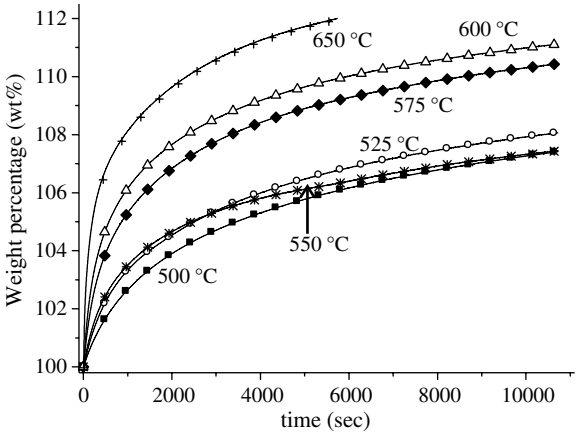

Fig. 4. Isotherms of CO_2 absorption on the CaAl-550 sample at different temperatures

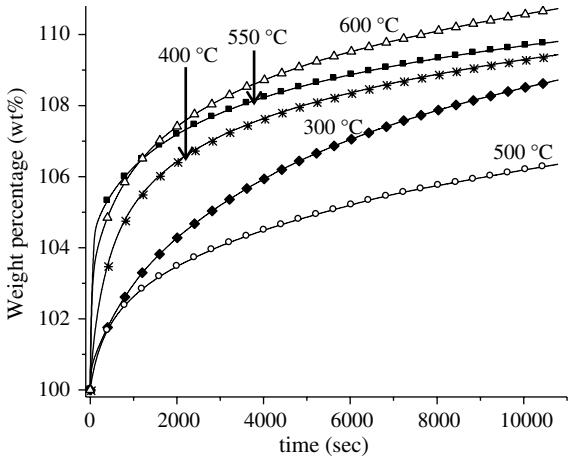

Fig. 5. Isotherms of CO_2 absorption on pure CaO at different temperatures

isothermal analysis performed at 500°C depicted the original exponential behavior, not the absorption-desorption isotherm observed for the CaAl-300 sample at the same temperature. Whereas the CaAl-300 sample only absorbed 0.8 wt% of CO_2 at 500°C, the CaAl-550 sample absorbed 7.4 wt% after 3 h. This means almost 10 times more CO_2. The CaAl-550 sample was activated at higher temperatures and the XRD results showed a fully crystalline structure conformed by CaO and $Ca_{12}Al_{14}O_{33}$, whereas no $CaCO_3$ was observed in this case. Therefore, the microstructure of this ceramic must be more stable and able to react with CO_2. In fact, the CO_2 absorption behavior is very similar to that presented by pure CaO (as described in the following). At 525°C, the isotherm was similar and the final CO_2 absorbed increased up to 8.0 wt%. However, isothermal experiment performed at 550°C presented a different behavior. The CO_2 absorption, at short times, increased from 500 to 550°C, but at long times the total CO_2 absorption at 550°C was less than that obtained at 525 and 500°C. In this case, because there is no weight loss, the phenomenon cannot be ascribed to absorption-desorption equilibrium. However, this atypical behavior has been already reported for gas absorption on different materials. For example, CO_2 absorption on alkaline ceramics Na_2ZrO_3, Li_5AlO_4 and Li_2CuO_2 (Ávalos-Rendón et al. 2009; Alcérreca-Corte et al. 2008; Palacios-Romero et al. 2009), or O_2 absorption on free-standing porous silicon (Cisneros et al. 2010). This effect has been associated to a sintering process, which decreases the surface area available for the gas absorption. Then, sintering must occur in this sample as well. In fact, because this behavior fits very well with the activation temperature of the sample (550°C), it must be assumed that on the isotherms performed at higher temperatures the sample is, at least, equally sintered than at 550°C. Finally, isotherms of the samples treated between 575 and 650°C showed exponential trends, absorbing up to 12.6 wt% of CO_2. In these cases, CO_2 absorption increased, although sintering must be enhanced. However, in these cases, sintering does not affect as importantly, because the bulk diffusion processes are becoming dominant, allowing high CO_2 absorptions (Ávalos-Rendón et al. 2009; Alcérreca-Corte et al. 2008; Palacios-Romero et al. 2009).

For comparison purposes, CaO was isothermically treated again under the same CO_2 atmosphere (Fig. 5). Here, the isotherms performed at 300 and 400°C presented exponential behaviors, as expected, absorbing more CO_2 at 400°C (9.4 wt%) than at 300°C (8.7 wt%). For the CaO sample, the atypical behavior attributed to the sintering process was again observed at 500°C, because CaO only absorbed 6.3 wt% of CO_2 at this temperature. Therefore, pure CaO sintered at a lower temperature than CaAl-550, which sintered at 550°C. The difference of the sintering temperature can be explained in terms of the chemical composition of each sample. The CaAl-550 sample is not pure CaO; it contains a secondary phase ($Ca_{12}Al_{14}O_{33}$) that must delay the sintering process, owing to variations of the thermal gradients of the sample. Finally, coming back to the isothermal experiments, CaO increased its CO_2 absorption at 550 and 600°C, in each case absorbing 9.8 and 10.7 wt%, respectively. Comparing, qualitatively, the isothermal experiments of CaAl-550 and CaO, both samples presented very similar behaviors and CO_2 absorption quantities. Hence, it seems that CO_2 absorption on the CaAl-550 sample occurs primarily on calcium oxide, and not on the $Ca_{12}Al_{14}O_{33}$ phase, which in fact does not affect the CO_2 absorption process.

Isothermal data obtained for CO_2 absorption on CaAl-550 were fitted to a first-order reaction, with respect to CaAl-550, because those experiments were carried out in a flow of excess CO_2 (Mosqueda et al. 2006):

$$\ln[\text{CaAl-550}] = -kt \tag{1}$$

Only the CaAl-550 sample was analyzed to eliminate, as much as possible, the influence of the sintering effect. Furthermore, only the first seconds of each isotherm were taken into account, because after that time an external layer of $CaCO_3$ is produced, and then the process is much slower, because it is diffusion-controlled (Ávalos-Rendón et al. 2009; Alcérreca-Corte et al. 2008; Palacios-Romero et al. 2009). Fig. 6 shows the plots of ln[CaAl-550] versus time (t) at different temperatures. The obtained rate constant values (k) are presented in Table 1 and compared to the values from CO_2 absorption on pure CaO, obtained by following the same procedure. Although the k values indicate that CaAl-550 sample absorbs CO_2 slower than CaO, both sets of values tend to increase as a function of temperature. Additionally, the difference between the two constants values is reduced as a function of temperature. These results strongly suggest that CO_2 absorption on CaAl-550 is positively altered by the presence of $Ca_{12}Al_{14}O_{33}$. Therefore, these results are in good agreement with previous reports mentioning that $Ca_{12}Al_{14}O_{33}$ plays an important role inhibiting the sintering process (Yang et al. 2009; Manovic and Anthony 2009; Li et al. 2009; Martavaltzi and Lemonidou 2008a, b; Lu et al. 2009, 2006; Florin and Harris 2009; Lisbona et al. 2010; Rodriguez et al. 2008).

J. Environ. Eng. 2011.137:1058-1065.

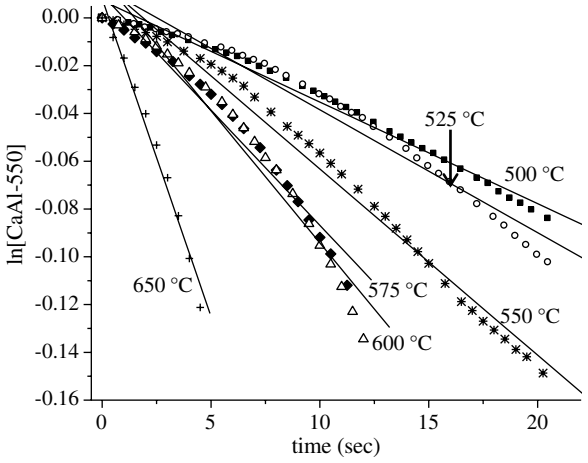

Fig. 6. Plot of ln[CaAl-550] versus time; only the first seconds were linearly adjusted, because in this time CO_2 absorption is the only activated process

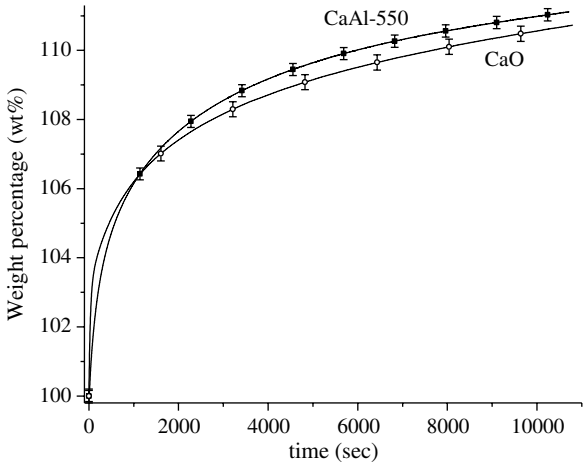

Fig. 7. Comparison of the CO_2 absorption isotherms of CaO and CaAl-550 samples at 600°C

Table 1. Rate Constant (k) Values for the CO_2 Absorption at Different Temperatures on CaAl-550 and Pure CaO

Temperature (°C)	CaAl-550		CaO	
	k (s^{-1})	R^2	k (s^{-1})	R^2
450	—	—	1.90×10^{-4}	0.9982
500	4.25×10^{-5}	0.9939	6.92×10^{-5}	0.9992
525	5.14×10^{-5}	0.9825	—	—
550	7.79×10^{-5}	0.9920	7.84×10^{-4}	0.9991
575	9.6×10^{-5}	0.9839	—	—
600	1.1×10^{-4}	0.9779	8.22×10^{-4}	0.9975
650	2.66×10^{-4}	0.9911	6.50×10^{-4}	0.9921

A further detailed examination of the CaAl-550 and CaO isotherms performed at the same temperature shows interesting results. Fig. 7 shows isotherms performed at 600°C for both materials. As has been elucidated from the k values, at the first moments (initial 20–30 s), CO_2 absorption on CaO is faster than on CaAl-550. However, a few minutes later (approximately 11,000 s), the isotherms intersect each other. Afterward, CaAl-550 absorbed more CO_2 than CaO. This effect may be attributed to a combination of different factors, such as surface area and thermal stability. CaO has twice the surface area (12.1 m^2/g) than CaAl-550 (6.2 m^2/g). Therefore, at the first moments, CaO has more surface area where CO_2 can be absorbed, retarding the CO_2 absorption diffusion-controlled process more than the CaAl-550 sample. However, at long times, the $Ca_{12}Al_{14}O_{33}$ phase should thermally stabilize the CaAl-550 sample, inhibiting its sintering and favoring the diffusion processes.

Based on all the previous results, the cyclability performance of the CaAl-550 sample was evaluated at different temperatures [500, 575, and 650°C, Fig. 8(a)] and times. It is clearly evident that at 500°C the CO_2 absorption-desorption process on the CaAl-550 sample was almost negligible. Although in the first cycle the CO_2 absorption was considerable (8.2 wt%), the temperature established for this experiment did not allow the CO_2 desorption, inhibiting further CO_2 absorption on the subsequent cycles. The sample recycled at 575°C presented very different behavior. At this temperature, the absorption-desorption process was completed. In the first cycle, the CO_2 absorption was equal to 9.8 wt%, without a desorption step. During cycles the sample presented a reasonable

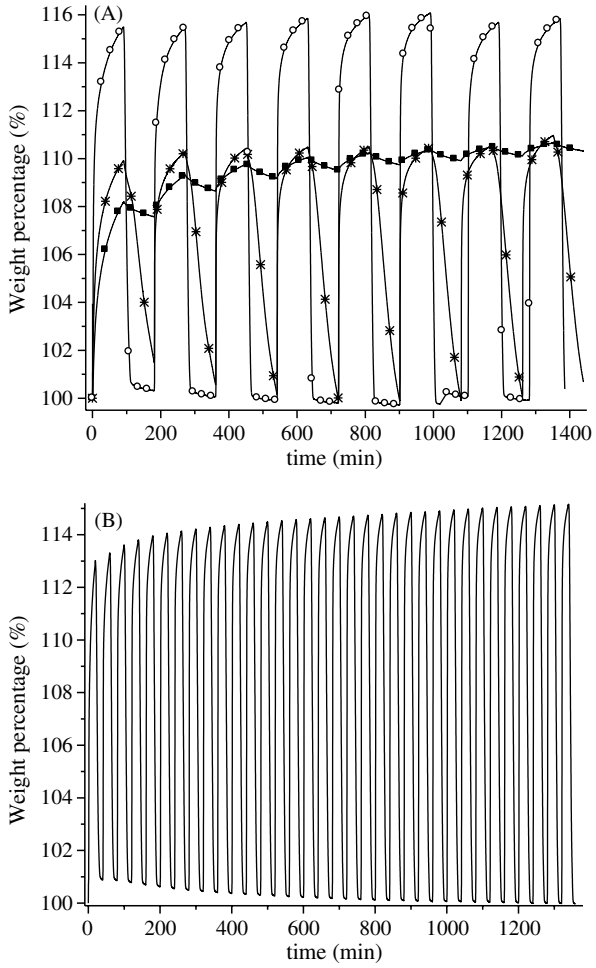

Fig. 8. (a) Cycle absorption-desorption performance of the CaAl-550 sample treated at different temperatures [500°C (■), 575°C (*), and 650°C (○)]; (b) cycle absorption-desorption performance of the CaAl-550 sample treated at 650°C, shortening the absorption-desorption times

stability on the absorption-desorption process, at approximately 10 ± 0.5 wt%. Finally, the sample treated at 650°C presented the best behavior. CO_2 absorption-desorption was stable, absorbing up to 16 wt% on each cycle. Not only was the CO_2 absorption faster

J. Environ. Eng. 2011.137:1058-1065.

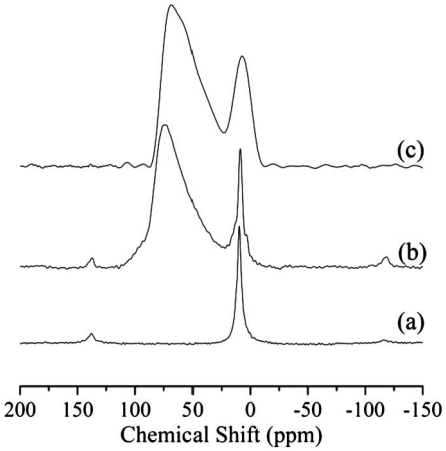

Fig. 9. ^{27}Al NMR spectra after CO_2 absorption-desorption cycles of (a) native CaAl sample; (b) CaAl-550; (c) CaAl-550

in this sample, as could be expected, but the desorption process was faster as well. Based on these results, the cyclability of the CaAl-550 sample was again evaluated at 650°C, but the absorption-desorption times were shortened to 20 min [Fig. 8(b)] to compare these results with previously published materials (Wu et al. 2008). During the first 10 cycles, the total CO_2 absorption efficiency increases from 12.4 to 14.9 wt%. After those cycles, the behavior remained constant (14.9–15.1 wt%). In this case, the efficiency did not decrease with increasing cycle numbers, as previously reported (Wu et al. 2008; Lu et al. 2006). This may be explained by two different factors. On one hand, both processes (absorption and desorption) were performed at the same temperature, 650°C. This must reduce sample sintering. On the other hand, because aluminum is homogeneously dispersed on the original ceramic, the $Ca_{12}Al_{14}O_{33}$ phase produced must also be uniformly dispersed, retarding the sintering process in a very efficient way.

In this context, ^{27}Al NMR spectra of Fig. 9 support that both CaAl-550 samples, activated and after the absorption-desorption cycles, present a significant amount of tetrahedral aluminum (broad peak close to 70 ppm). Actually, the native Ca-Al-CO_3 sample presents only a peak near 5 ppm, which is attributed to aluminum coordinated to six oxygen neighbors (Lippmaa et al. 1986; Fyfe et al. 1985). The narrowness of the peak is consistent with a hydrated sample where the electronic charge distribution in aluminum's local environment is homogeneously distributed. With activation (sample CaAl-550), as shown by XRD, layered structure of hydrocalumite collapses, and a mixture of oxides emerges where a significant amount of aluminum ions are in tetrahedral coordination and the octahedral aluminum is no longer completely symmetric, because of the absence of water molecules. After the absorption-desorption CO_2 cycles, tetrahedral aluminum species remain present and octahedral aluminum sites are slightly modified, as suggested by a broader peak at 5.2 ppm. It is difficult to clarify why octahedral sites are modified, but a possibility is that quadrupolar interaction becomes stronger owing to dispersion of the $Ca_{12}Al_{14}O_{33}$ phase. The peak attributable to tetrahedral aluminum species is also modified with absorption-desorption CO_2 cycles. A shift toward stronger field was observed, if it is compared with the original spectra. This result supports the fact that the material's structure is not exactly the same at the end of absorption. Aluminum migration in mixed oxide could occur as a consequence of dispersion of $Ca_{12}Al_{14}O_{33}$.

Finally, backscattered electron micrographs of the activated CaAl-550 sample before and after the absorption-desorption cycles

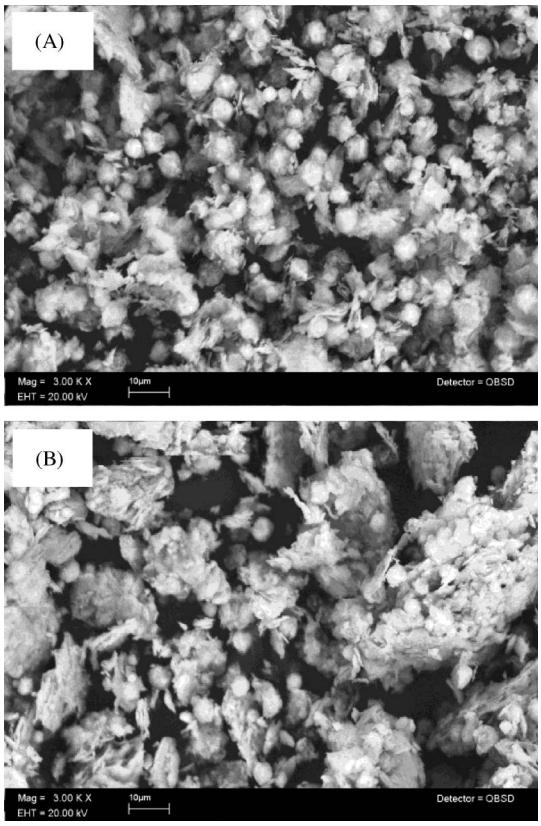

Fig. 10. Backscattered electron images of the CaAl-550 sample after (a) the thermal activation; (b) CO_2 absorption-desorption cycles

are shown in Fig. 10. The activated CaAl-550 sample presented a combination of two different morphologies relatively dispersed; semispherical and flakelike particles [Fig. 10(a)]. The average particle sizes of these structures were 8 ± 1 μm and 10 ± 1 μm for the semispherical and flakelike particles, respectively. Afterward, when the CaAl-550 sample was cycled its morphology slightly varied [Fig. 10(b)]. The two primary morphologies were preserved, but in this case both tend to produce agglomerates equal to or greater than 30 μm. The interaction observed among the particles may be explained in terms of the expansion-contraction processes produced during the CO_2 absorption-desorption, although the morphological changes did not alter the CO_2 absorption efficiency during the cycling process, as shown previously.

Conclusions

A Ca/Al layered double hydroxide (hydrocalumite, $[Ca_2Al(OH)_6]_2CO_3 \cdot mH_2O$) was synthesized by precipitation and then thermally activated at two different temperatures (300 and 550°C). Different CO_2 absorption experiments were performed over these two activated samples, and results were compared with similar experiments performed over a CaO sample. The experiments showed that CaAl-550 sample possesses good properties as CO_2 sorbent, even compared with CaO. It was found that both materials (CaAl-550 and CaO) seem to have similar kinetic behavior, and the presence of $Ca_{12}Al_{14}O_{33}$ on the CaAl-550 sample did not reduce or interfere with the CO_2 capture. Moreover, when the CO_2 absorption-desorption cyclability was analyzed, the CaAl-550 sample presented some interesting properties, such as the CO_2 absorption-desorption efficiencies at short times, and a high thermal stability after more than 30 cycles. In fact, the

J. Environ. Eng. 2011.137:1058-1065.

improvements observed on efficiency and thermal stability were attributed to the aluminum-containing phase, $Ca_{12}Al_{14}O_{33}$, using different characterization analyses such as NMR and SEM.

Acknowledgments

Authors thank the technical assistance of A. Tejeda, G. Zedillo, and O. Novelo. This work was performed into the PUNTA-IMPULSA framework and financially supported by ICyT-DF-179/2009 and CONACyT-60980 projects.

References

Alcérreca-Corte, I., Fregoso-Israel, E., and Pfeiffer, H. (2008). "CO_2 absorption on Na_2ZrO_3: A kinetic analysis of the chemisorption and diffusion processes." *J. Phys. Chem. C*, 112(16), 6520–6525.

Ávalos-Rendón, T., Casa-Madrid, J., and Pfeiffer, H. (2009). "Thermochemical capture of carbon dioxide on lithium aluminates ($LiAlO_2$ and Li_5AlO_4): A new option for the CO_2 absorption." *J. Phys. Chem. A*, 113(25), 6919–6923.

Bhatia, S. K., and Perlmutter, D. D. (1983). "Effect of the product layer on the kinetics of the CO_2-lime reaction." *AlChE J.*, 29, 79–86.

Chen, J., Loo, L. S., and Wang, K. (2008). "High-pressure CO_2 adsorption on a polymer-derived carbon molecular sieve." *J. Chem. Eng. Data*, 53(1), 2–4.

Chen, Y. T., Karthik, M., and Bai, H. (2009). "Modification of CaO by organic alumina precursor for enhancing cyclic capture of CO_2 greenhouse gas." *J. Environ. Eng.*, 135(6), 459–464.

Choi, S., Drese, J. H., and Jones, C. W. (2009). "Adsorbent materials for carbon dioxide capture from large anthropogenic point sources." *ChemSusChem*, 2, 796–854.

Cisneros, R., Pfeiffer, H., and Wang, C. (2010). "Oxygen absorption in free-standing porous silicon: A structural, optical and kinetic analysis." *Nano. Res. Lett.*, 5(4), 686–691.

Díaz, E., Muñoz, E., Vega, A., and Ordónez, S. (2008). "Enhancement of the CO_2 retention capacity of X zeolites by Na- and Cs-treatments." *Chemosphere*, 70(8), 1375–1382.

Florin, N. H., and Harris, A. T. (2009). "Reactivity of CaO derived from nano-sized $CaCO_3$ particles through multiple CO_2 capture-and-release cycles." *Chem. Eng. Sci.*, 64(2), 187–191.

Friedmann, S. J. (2007). "Geological carbon dioxide sequestration." *Elements*, 3, 179–184.

Fyfe, C. A., et al. (1985). "Detailed interpretation of the ^{29}Si and ^{27}Al high-field *MAS* NMR spectra of zeolites offretite and omega." *Zeolites*, 5(3), 179–186.

Kirkpatrick, R. J., Yu, P., Hou, H., and Kim, Y. (1999). "Interlayer structure, anion dynamics, and phase transitions in mixed-metal layered hydroxides: Variable temperature ^{35}Cl NMR spectroscopy of hydrotalcite and Ca-aluminate hydrate (hydrocalumite)." *Am. Mineral.*, 84, 1186–1190.

Li, Z. S., Fang, F., and Cai, N. S. (2009). "CO_2 capture from flue gases using three Ca-based sorbents in a fluidized bed reactor." *J. Environ. Eng.*, 135(6), 418–425.

Lima, E., Laspéras, M., de Ménorval, L. C., Tichit, D., and Fajula, F. (2004). "Characterization of basic catalysts by the use of nitromethane as NMR probe molecule and reactant." *J. Catal.*, 223(1), 28–35.

Lippmaa, E., Samoson, A., and Magi, M. (1986). "High-resolution aluminum-27 NMR of aluminosilicates." *J. Am. Chem. Soc.*, 108(8), 1730–1735.

Liu, W., Low, N. W. L., Feng, B., Wang, G., and Da Costa, J. D. (2010). "Calcium precursors for the production of CaO sorbents for multicycle CO_2 capture." *Environ. Sci. Technol.*, 44(2), 841–847.

Lisbona, P., Martínez, A., Lara, Y., and Romeo, L. M. (2010). "Integration of carbonate CO_2 capture cycle and coal-fired power plants. A comparative study of different sorbents." *Energy Fuels*, 24(1), 728–736.

Lu, H., Reddy, E. P., and Smirniotis, G. (2006). "Calcium oxide based sorbents for capture of carbon dioxide at high temperatures." *Ind. Eng. Chem. Res.*, 45(11), 3944–3949.

Lu, D. Y., Hughes, R. W., Anthony, E. J., and Manovic, V. (2009). "Sintering and reactivity of $CaCO_3$-based sorbents for in situ CO_2 capture in fluidized beds under realistic calcination conditions." *J. Environ. Eng.*, 135(6), 404–410.

Lwin, Y., and Abdullah, F. (2009). "High temperature adsorption of carbon dioxide on Cu–Al hydrotalcite-derived mixed oxides: Kinetics and equilibria by thermogravimetry." *J. Therm. Anal. Calorim.*, 97(3), 885–889.

Macario, A., Katovic, A., Giordano, G., Iucolano, F., and Caputo, D. (2005). "Synthesis of mesoporous materials for carbon dioxide sequestration." *Microporous Mesoporous Mater.*, 81(1-3), 139–147.

Maceiras, R., Alves, S. S., Cancela, M. A., and Alvarez, E. (2008). "Effect of bubble contamination on gas-liquid mass transfer coefficient on CO_2 absorption in amine solutions." *Chem. Eng. J.*, 137(2), 422–427.

Manovic, V., and Anthony, E. J. (2009). "CaO-based pellets supported by calcium aluminate cements for high-temperature CO_2 capture." *Environ. Sci. Technol.*, 43(18), 7117–7122.

Manovic, V., and Anthony, E. J. (2010). "CO_2 carrying behavior of calcium aluminate pellets under high-temperature/high-CO_2 concentration calcination conditions." *Ind. Eng. Chem. Res.*, 49, 6919–6922.

Martavaltzi, C. S., and Lemonidou, A. A. (2008a). "Development of new CaO based sorbent materials for CO_2 removal at high temperature." *Microporous Mesoporous Mater.*, 110(1), 119–127.

Martavaltzi, C. S., and Lemonidou, A. A. (2008b). "Parametric study of the CaO-$Ca_{12}Al_{14}O_{33}$ synthesis with respect to high CO_2 sorption capacity and stability on multicycle operation." *Ind. Eng. Chem. Res.*, 47(23), 9537–9543.

Mosqueda, H. A., Vazquez, C., Bosch, P., and Pfeiffer, H. (2006). "Chemical sorption of carbon dioxide (CO_2) on lithium oxide (Li_2O)." *Chem. Mater.*, 18(9), 2307–2310.

Nair, B. N., Yamaguchi, T., and Kawamura, H. (2004). "Processing of lithium zirconate for applications in carbon dioxide separation: Structure and properties of the powders." *J. Am. Ceram. Soc.*, 87(1), 68–74.

Nair, B. N., Burwood, R. P., Goh, V. J., Nakagawa, K., and Yamaguchi, T. (2009). "Lithium based ceramic materials and membranes for high temperature CO_2 separation." *Prog. Mater. Sci.*, 54(5), 511–541.

Nomura, K., Tokumistu, K., Hayakawa, T., and Homonnay, Z. (2000). "The influence of mechanical treatment on the absorption of CO_2 by perovskite oxides." *J. Radiol. Nucl. Chem.*, 246(1), 69–77.

Ochoa-Fernández, E., Zhao, T., Rønning, M., and Chen, D. (2009). "Effects of steam addition on the properties of high temperature ceramic CO_2 acceptors." *J. Environ. Eng.*, 135(6), 397–403.

Palacios-Romero, L. M., Lima, E., and Pfeiffer, H. (2009). "Structural analysis and CO_2 chemisorption study on non-stoichiometric lithium cuprates ($Li_{2+x}CuO_{2+x/2}$)." *J. Phys. Chem. A*, 113(1), 193–198.

Park, S. W., Cho, H. B., and Sohn, I. (2002). "CO_2 absorption into w/o emulsion with aqueous amine liquid droplets." *J. Sep. Sci.*, 37, 639–661.

Pawlesa, J., Zukal, A., and Cejka, J. (2007). "Synthesis and adsorption investigations of zeolites MCM-22 and MCM-49 modified by alkali metal cations." *Adsorp. J. Int. Adsorp. Soc.*, 13, 257–265.

Preda, G., Pacchioni, G., Chiesa, M., and Giamello, E. (2009). "The reactivity of CO_2 with K atoms adsorbed on MgO." *Phys. Chem. Chem. Phys.*, 11(37), 8156–8164.

Rodriguez, N., Alonso, M., Grasa, M., and Abanades, J. C. (2008). "Heat requirements in a calciner of $CaCO_3$ integrated in a CO_2 capture system using CaO." *Chem. Eng. J.*, 138(1-3), 148–154.

Romeo, L. M., Bolea, I., and Escosa, J. M. (2008). "Integration of power plant and amine scrubbing to reduce CO_2 capture costs." *Appl. Therm. Eng.*, 28(8-9), 1039–1046.

Rouquerol, F., Rouquerol, J., and Sing, K. (1999). *Adsorption by powders and porous solids: Principles, methodology and applications*, Academic Press, 97.

Segni, R., Allali, N., Vieille, L., Taviot-Guého, C., and Leroux, F. (2006). "Hydrocalumite-type materials: 2. Local order into $Ca_2Fe(OH)_6(CrO_4^{2-})_{0.5} \cdot nH_2O$ in temperature studied by X-ray absorption and Mössbauer spectroscopies." *J. Phys. Chem. Solids*, 67(5-6), 1043–1047.

J. Environ. Eng. 2011.137:1058-1065.

Seo, Y., Jo, S. H., Ryu, C. K., and Yi, C. K. (2009). "Effect of reaction temperature on CO_2 capture using potassium-based solid sorbent in bubbling fluidized-bed reactor." *J. Environ. Eng.*, 135(6), 473–477.

Wu, S. F., Li, Q. H., Kim, J. N., and Yi, K. B. (2008). "Properties of a nano CaO/Al_2O_3 CO_2 sorbent." *Ind. Eng. Chem. Res.*, 47(1), 180–184.

Yang, Z. H., Zhao, M., Florin, N. H., and Harris, A. T. (2009). "Synthesis and characterization of CaO nanopods for high temperature CO_2 capture." *Ind. Eng. Chem. Res.*, 48(24), 10765–10770.

Yavuz, C. T., et al. (2009). "Markedly improved CO_2 capture efficiency and stability of gallium substituted hydrotalcites at elevated temperatures." *Chem. Mater.*, 21(15), 3473–3475.

J. Environ. Eng. 2011.137:1058-1065.